



## ACTIVE GALACTIC NUCLEI

# Multi-wavelength characterization of Fermi blazars of uncertain type

VAIDEHI S. PALIYA<sup>ID</sup>

Aryabhatta Research Institute of Observational Sciences (ARIES), Manora Peak, Nainital 263001, India.  
E-mail: vaidehi.s.paliya@gmail.com

MS received 24 November 2021; accepted 13 December 2021

**Abstract.** One of the major challenges in the research of jetted active galactic nuclei (AGN) is the completeness of the source catalogs released using the  $\gamma$ -ray data taken from the *Fermi*-large area telescope (LAT). There are about  $\sim 30\%$  of the *Fermi*-LAT detected blazars whose classification is yet to be ascertained, so-called blazars candidates of uncertain (BCU) type, thereby hampering the attempts made to explore the problems associated with relativistic jets. Using the results obtained in a recent study focused on the optical spectroscopic and multi-band properties of a large sample of *Fermi* blazars, this work classifies 57 BCUs presents in the fourth catalog of the *Fermi*-LAT detected AGN as flat-spectrum radio quasars (FSRQs) and 96 as BL Lac type sources. In the  $\gamma$ -ray luminosity versus  $\gamma$ -ray photon index plane, these newly classified blazars occupy regions populated by their known counterparts. The Compton dominance and accretion luminosity normalized by the Eddington one, for BCUs appear to follow the positive correlation already identified for known blazars. These observations suggest that Compton dominance can be used as a proxy for the accretion rate, thus supporting the Compton dominance-based blazar classification scheme.

**Keyword.** Methods: data analysis—gamma rays: general—galaxies: active—galaxies: jets.

## 1. Introduction

Active galactic nuclei hosting powerful relativistic jets aligned close to the line of sight to the observer are called blazars. Some of the defining properties of blazars are temporal and spectral flux variability, highly polarized radio and optical radiation, a flat radio spectrum, and superluminal motion. Blazars are classified as flat-spectrum radio quasars (FSRQs) and BL Lac objects with the former exhibiting broad and strong emission lines (rest-frame equivalent width  $>5 \text{ \AA}$ ) in their optical spectra (Stickel *et al.* 1991).

Blazars are strong  $\gamma$ -ray emitters and dominate the extragalactic high-energy  $\gamma$ -ray sky (cf. Ajello *et al.* 2020). Among the thousands of blazars detected with the *Fermi*-large area telescope (LAT), there are still  $\sim 30\%$  whose classification, i.e., FSRQs or BL Lacs, is unknown (Ajello *et al.* 2020). This is either due to lack of optical spectroscopy or due to extremely poor signal-to-noise

ratio of the optical spectrum even if it is available. Such objects are called blazar candidates of uncertain type or BCU type (Ackermann *et al.* 2011). Several multi-frequency properties of BCUs are found to be similar to blazars, however, due to the lack of classification, these cannot be used to study various crucial research problems, e.g., blazar luminosity function. Optical spectroscopic followup of some of the BCUs has led to the identification of peculiar objects that have provided new insights on blazar phenomenon, e.g., the first  $z > 3$   $\gamma$ -ray detected BL Lac object (Paliya *et al.* 2020), thus highlighting the importance of characterizing BCUs. To this purpose, various spectroscopic campaigns have been carried out to classify these objects (Peña-Herazo *et al.* 2020).

Recently, Paliya *et al.* (2021) analyzed publicly available optical spectra of  $>1000$  blazars included in the second data release of the fourth catalog of the *Fermi*-LAT detected AGN (4LAC-DR2; Ajello *et al.* 2020) and reported their black hole mass ( $M_{\text{BH}}$ ), and accretion disk luminosity ( $L_{\text{disk}}$ ). For sources with broad emission lines, these quantities were calculated following the single epoch virial relations (Shen *et al.*

This article is part of the Special Issue on “Astrophysical Jets and Observational Facilities: A National Perspective”.

2011). On the other hand,  $M_{\text{BH}}$  values were estimated from the stellar velocity dispersion for blazars whose optical spectra are dominated by the host galaxy absorption features. By fitting their radio-to- $\gamma$ -ray spectral energy distributions (SEDs) with polynomial functions, Paliya *et al.* (2021) also measured the ratio of the high- and low-energy peak luminosities, so-called the Compton dominance, and determined a strong correlation between the accretion rate in the Eddington unit and Compton dominance.

This work takes benefit of the physical parameters reported in Paliya *et al.* (2021) to classify BCUs present in the 4LAC-DR2 catalog. Section 2 describes the sample adopted in this study. Results are presented in Section 3 and summarized in Section 4.

## 2. Sample

The 4LAC-DR2 catalog contains 1499 BCUs including 1292 without the redshift information. Furthermore, Paliya *et al.* (2021) studied the optical spectra of 1020 4LAC-DR2 blazars, including BCUs, by taking the advantage of recent advancements in optical spectroscopy, e.g., sixteenth data release of the Sloan Digital Sky Survey (SDSS-DR16; Ahumada *et al.* 2020). Therefore, it is likely that many *Fermi*-BCUs might be present in the sample of Paliya *et al.* (2021). With this in mind, 1499 BCUs from 4LAC-DR2 were cross-matched with the Paliya *et al.* (2021) sample. This exercise has led to the identification of 70 BCUs whose optical spectra reveal broad/narrow emission lines. Additionally, 83 BCUs were also found whose optical spectra are dominated by the absorption features arising from the host galaxy.

## 3. Results

### 3.1 Emission and absorption line BCUs

There are 153 BCUs present in the Paliya *et al.* (2021) sample whose optical spectra show prominent emission/absorption lines. There are 83 of them whose optical spectra do not exhibit any emission lines and are rather dominated by absorption features. Paliya *et al.* (2021) modeled these spectra with penalized Pixel Fitting software (pPXF; Cappellari & Emsellem 2004) to determine the stellar velocity dispersion. Following the empirical relations of Gültekin *et al.* (2009),  $M_{\text{BH}}$  values were measured. Furthermore, Paliya *et al.* (2021) also computed the  $3\sigma$  upper limit in  $L_{\text{disk}}$  and the Compton dominance from the broadband SEDs of these sources.

For all of the 83 sources, only  $3\sigma$  upper limit in the accretion rate could be measured, indicating a radiatively inefficient accretion process and supporting the BL Lac nature of these sources (Ghisellini *et al.* 2011). The left panel of Figure 1 shows the optical spectrum of one such BCU. Table 1 reports these 83 objects along with their central engine parameters.

There are 70 *Fermi* BCUs whose optical spectra reveal strong/faint broad emission lines. An example is demonstrated in the right panel of Figure 1. Since an equivalent width-based blazar classification is likely not physically motivated (cf. Ghisellini *et al.* 2011), Paliya *et al.* (2021) proposed another scheme. An FSRQ is a blazar with an accretion rate  $\geq 1\%$  of Eddington value and Compton dominance  $\geq 1$ . On the other hand, sources with the accretion rate  $<1\%$  of Eddington one and Compton dominance  $<1$  can be classified as BL Lac objects. Following this

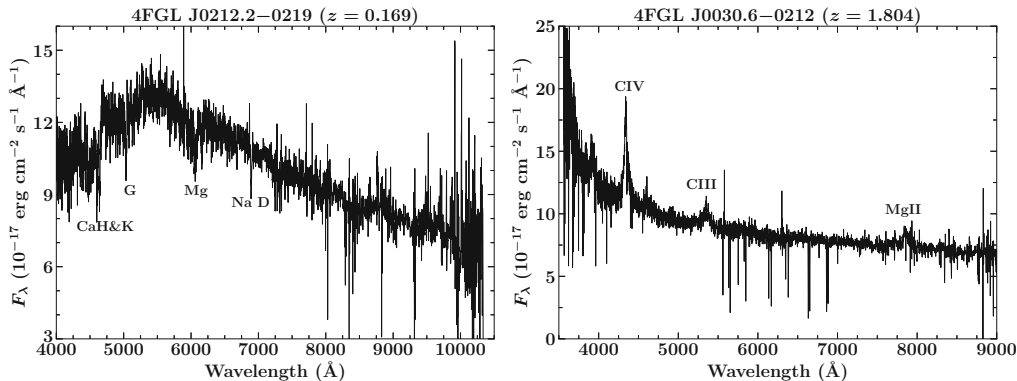


**Figure 1.** Optical spectra of *Fermi* BCUs reported in the SDSS-DR16. The left panel highlights the absorption features arising from the host galaxy of the BCU 4FGL J0212.2–0219. The lack of emission lines suggests a radiatively inefficient accretion which in turn hints this object to be of BL Lac type. On the other hand, prominent emission lines can be seen in the right panel, suggesting the BCU 4FGL J0030.6–0212 to be of FSRQ type.

**Table 1.** The list of *Fermi* BCUs whose optical spectra exhibit prominent absorption features, indicating them to belong to the BL Lac class of blazars. All of the parameters are adopted from Paliya *et al.* (2021). Both,  $M_{\text{BH}}$  (in  $M_{\odot}$ ) and  $3\sigma$  upper limit in  $L_{\text{disk}}$  (in erg s $^{-1}$ ) values are in log-scale. The second last column reports the Compton dominance and the last one refers to the proposed classification (bll).

4FGL name	$z$	$M_{\text{BH}}$	$L_{\text{disk,UL}}$	$L_{\text{disk,UL}}/L_{\text{Edd}}$	CD
J0006.4+0135	0.787	$9.33 \pm 0.33$	44.62	$1.50 \times 10^{-3}$	0.69
J0029.4+2051	0.367	$9.01 \pm 0.18$	43.97	$7.02 \times 10^{-4}$	0.48
J0049.1+4223	0.302	$9.23 \pm 0.16$	43.79	$2.79 \times 10^{-4}$	0.49
J0102.4+0942	0.421	$8.62 \pm 0.33$	44.31	$3.77 \times 10^{-3}$	0.55
J0109.3+2401	0.493	$8.22 \pm 0.45$	44.28	$8.83 \times 10^{-3}$	0.29
J0119.6+4158	0.109	$8.63 \pm 0.11$	42.98	$1.72 \times 10^{-4}$	0.38
J0121.8–3916	0.39	$8.58 \pm 0.15$	44.39	$4.97 \times 10^{-3}$	0.44
J0135.1+0255	0.372	$8.72 \pm 0.19$	44.01	$1.50 \times 10^{-3}$	0.62
J0154.3–0236	0.082	$9.12 \pm 0.14$	43.21	$9.46 \times 10^{-5}$	0.21
J0204.3+2417	0.21	$9.46 \pm 0.18$	43.49	$8.24 \times 10^{-5}$	0.34
J0211.1–0646	0.194	$8.92 \pm 0.16$	43.45	$2.61 \times 10^{-4}$	0.13
J0212.2–0219	0.169	$7.9 \pm 0.14$	43.35	$2.17 \times 10^{-3}$	0.2
J0238.7+2555	0.584	$9.63 \pm 0.21$	44.56	$6.55 \times 10^{-4}$	0.39
J0301.0–1652	0.278	$9.05 \pm 0.16$	44.01	$7.02 \times 10^{-4}$	0.18
J0312.4–3221	0.067	$8.73 \pm 0.14$	42.57	$5.32 \times 10^{-5}$	0.09
J0325.3+3332	0.128	$9.2 \pm 0.16$	43.1	$6.11 \times 10^{-5}$	0.28
J0500.2+5237	0.123	$9.19 \pm 0.17$	43.92	$4.13 \times 10^{-4}$	0.13
J0600.3+1244	0.084	$8.83 \pm 0.14$	43.15	$1.61 \times 10^{-4}$	0.25
J0602.0+5315	0.052	$9.55 \pm 0.18$	42.88	$1.64 \times 10^{-5}$	0.35
J0602.7–0007	0.118	$9.48 \pm 0.19$	43.34	$5.57 \times 10^{-5}$	0.45
J0620.7+2643	0.133	$9.56 \pm 0.17$	43.5	$6.70 \times 10^{-5}$	0.11
J0709.2–1527	0.142	$9.74 \pm 0.19$	43.68	$6.70 \times 10^{-5}$	0.15
J0733.4+5152	0.065	$8.92 \pm 0.11$	42.53	$3.13 \times 10^{-5}$	0.06
J0815.9+2951	0.331	$8.74 \pm 0.17$	43.86	$1.01 \times 10^{-3}$	0.3
J0830.0+5231	0.206	$8.79 \pm 0.16$	43.53	$4.23 \times 10^{-4}$	0.44
J0836.9+5833	0.611	$8.21 \pm 0.44$	44.88	$3.60 \times 10^{-2}$	0.83
J0842.7+6656	0.121	$8.4 \pm 0.14$	43.02	$3.21 \times 10^{-4}$	0.3
J0922.6+4454	0.467	$7.43 \pm 0.65$	44.06	$3.28 \times 10^{-2}$	4.57
J0930.5+5132	0.189	$8.37 \pm 0.17$	43.15	$4.64 \times 10^{-4}$	0.16
J0937.9–1434	0.287	$9.47 \pm 0.19$	43.94	$2.27 \times 10^{-4}$	0.62
J0952.8+0712	0.574	$9.25 \pm 0.23$	44.32	$9.04 \times 10^{-4}$	0.98
J1008.0+0028	0.098	$9.55 \pm 0.19$	43.28	$4.13 \times 10^{-5}$	0.56
J1008.8–3139	0.534	$9.23 \pm 0.32$	44.96	$4.13 \times 10^{-3}$	1.78
J1012.7+4228	0.365	$9.5 \pm 0.25$	44.24	$4.23 \times 10^{-4}$	0.39
J1017.3+5204	0.379	$7.52 \pm 0.39$	44.09	$2.86 \times 10^{-2}$	0.51
J1017.4+2538	0.417	$8.5 \pm 0.31$	44.08	$2.92 \times 10^{-3}$	0.43
J1028.3+3108	0.24	$8.79 \pm 0.28$	44.14	$1.72 \times 10^{-3}$	0.35
J1033.7+3708	0.448	$8.79 \pm 0.25$	44.12	$1.64 \times 10^{-3}$	0.59
J1046.0+5448	0.249	$8.23 \pm 0.13$	43.63	$1.93 \times 10^{-3}$	0.43
J1052.3+0818	0.223	$8.85 \pm 0.15$	43.63	$4.64 \times 10^{-4}$	0.27
J1121.3–0011	0.099	$9.47 \pm 0.17$	43.15	$3.68 \times 10^{-5}$	0.15
J1129.5+3034	0.68	$8.99 \pm 0.66$	44.93	$6.70 \times 10^{-3}$	0.62
J1132.2–4736	0.229	$8.79 \pm 0.11$	43.83	$8.43 \times 10^{-4}$	0.3
J1158.9+0818	0.291	$8.4 \pm 0.16$	43.89	$2.38 \times 10^{-3}$	0.45
J1208.4+6121	0.275	$8.94 \pm 0.18$	43.85	$6.25 \times 10^{-4}$	0.19
J1241.3+4236	0.619	$8.71 \pm 0.41$	44.62	$6.25 \times 10^{-3}$	1.51
J1310.6+2449	0.226	$8.8 \pm 0.18$	43.46	$3.52 \times 10^{-4}$	0.33

**Table 1.** Continued.

4FGL name	$z$	$M_{\text{BH}}$	$L_{\text{disk,UL}}$	$L_{\text{disk,UL}}/L_{\text{Edd}}$	CD
J1336.2+2053	0.628	$8.01 \pm 0.7$	44.6	$2.99 \times 10^{-2}$	0.83
J1340.1+3857	0.246	$9.97 \pm 0.22$	43.45	$2.32 \times 10^{-5}$	0.5
J1351.4–1529	0.285	$8.63 \pm 0.16$	44.41	$4.64 \times 10^{-3}$	0.55
J1356.2–1726	0.075	$9.03 \pm 0.14$	42.93	$6.11 \times 10^{-5}$	0.19
J1400.2–4010	0.203	$8.93 \pm 0.13$	43.2	$1.43 \times 10^{-4}$	0.21
J1416.1+1320	0.247	$7.57 \pm 0.34$	43.47	$6.11 \times 10^{-3}$	0.4
J1439.5–2525	0.16	$9.06 \pm 0.14$	43.24	$1.16 \times 10^{-4}$	0.28
J1439.9–3953	0.3	$8.8 \pm 0.16$	43.83	$8.24 \times 10^{-4}$	0.3
J1455.4–3654	0.095	$9.55 \pm 0.17$	43.68	$1.04 \times 10^{-4}$	0.12
J1544.3–0649	0.171	$9.41 \pm 0.2$	43.64	$1.31 \times 10^{-4}$	0.51
J1545.8–2336	0.121	$9.1 \pm 0.17$	43.33	$1.31 \times 10^{-4}$	0.32
J1559.8–2525	0.416	$9.05 \pm 0.16$	44.2	$1.09 \times 10^{-3}$	1.02
J1606.9+5919	0.132	$8.94 \pm 0.13$	43.12	$1.16 \times 10^{-4}$	0.12
J1612.2+2828	0.053	$8.22 \pm 0.1$	42.51	$1.50 \times 10^{-4}$	0.05
J1623.4+0858	0.533	$8.18 \pm 0.35$	44.37	$1.19 \times 10^{-2}$	0.28
J1640.9+1143	0.078	$9.71 \pm 0.18$	43.06	$1.72 \times 10^{-5}$	0.28
J1706.8+3004	0.704	$9.45 \pm 0.5$	44.81	$1.76 \times 10^{-3}$	0.39
J1707.5+1649	0.291	$9.41 \pm 0.31$	43.92	$2.49 \times 10^{-4}$	0.44
J1725.4+5254	0.061	$8.57 \pm 0.11$	42.6	$8.24 \times 10^{-5}$	0.09
J1808.8+3522	0.141	$9.36 \pm 0.18$	43.49	$1.04 \times 10^{-4}$	0.29
J1814.0+3828	0.275	$9.14 \pm 0.16$	43.78	$3.36 \times 10^{-4}$	0.46
J1831.9+3820	0.216	$9.1 \pm 0.15$	43.62	$2.55 \times 10^{-4}$	0.21
J1838.4–6023	0.121	$9.29 \pm 0.16$	43.56	$1.43 \times 10^{-4}$	0.1
J1842.4–5840	0.421	$8.9 \pm 0.28$	44.37	$2.27 \times 10^{-3}$	0.31
J1858.3+4321	0.136	$9.34 \pm 0.15$	43.31	$7.18 \times 10^{-5}$	0.09
J1929.4+6146	0.212	$9.8 \pm 0.19$	43.66	$5.57 \times 10^{-5}$	0.38
J1954.9–5640	0.221	$8.37 \pm 0.13$	44.08	$3.95 \times 10^{-3}$	0.14
J2148.9–0121	0.203	$8.79 \pm 0.14$	43.44	$3.44 \times 10^{-4}$	0.32
J2150.7–1750	0.185	$8.88 \pm 0.16$	43.56	$3.68 \times 10^{-4}$	0.34
J2159.1–2840	0.271	$8.31 \pm 0.21$	44.02	$3.95 \times 10^{-3}$	0.5
J2224.5+0353	0.293	$8.28 \pm 0.25$	43.93	$3.44 \times 10^{-3}$	0.21
J2226.6+0210	0.45	$9.22 \pm 0.3$	44.29	$9.04 \times 10^{-4}$	0.11
J2228.5+2211	0.71	$8.61 \pm 0.69$	44.83	$1.28 \times 10^{-2}$	0.42
J2236.6+3706	0.235	$8.92 \pm 0.18$	43.97	$8.63 \times 10^{-4}$	0.2
J2250.4+1748	0.344	$8.32 \pm 0.12$	43.84	$2.55 \times 10^{-3}$	13.49
J2316.9–5210	0.646	$9.44 \pm 0.23$	44.66	$1.28 \times 10^{-3}$	0.43

classification scheme, 57 emission line BCUs turned out to be FSRQs and 13 as BL Lac sources (see Table 2). As also discussed in Paliya *et al.* (2021), sources with accretion rate  $\approx 1\%$  and Compton dominance  $\approx 1$  may belong to the peculiar class of masquerading BL Lac objects<sup>1</sup> (Giommi *et al.* 2013).

<sup>1</sup>Masquerading BL Lac objects are proposed to be radiatively efficient accreting systems similar to FSRQs. However, their optical spectra do not exhibit broad emission lines due to strong Doppler boosting, hence misclassified as BL Lac sources.

### 3.2 A comparison with known FSRQs and BL Lac objects

In the left panel of Figure 2, the BCUs classified in this work are plotted in the  $\gamma$ -ray luminosity and  $\gamma$ -ray photon index diagram. For a comparison, known FSRQs and BL Lac objects present in the 4LAC-DR2 catalog are also shown. As can be seen, BCUs classified as FSRQs occupy a region populated mainly by known FSRQs. Similar results are obtained for objects

**Table 2.** The list of *Fermi* BCUs whose optical spectra exhibit broad emission lines.

4FGL name	$z$	$M_{\text{BH}}$	$L_{\text{disk}}$	$L_{\text{disk}}/L_{\text{Edd}}$	CD	Classification
J0013.6+4051	0.256	$7.02 \pm 0.78$	$43.14 \pm 0.21$	0.010	0.46	bll
J0014.3−0500	0.791	$7.93 \pm 0.18$	$44.93 \pm 0.03$	0.077	2.75	fsrq
J0023.7−6820	0.354	$8.01 \pm 0.2$	$45.41 \pm 0.05$	0.193	1.02	fsrq
J0030.6−0212	1.804	$8.66 \pm 0.28$	$45.98 \pm 0.02$	0.161	11.22	fsrq
J0036.9+1832	1.595	$8.0 \pm 0.09$	$45.7 \pm 0.04$	0.386	7.76	fsrq
J0040.9+3203	0.632	$7.17 \pm 0.19$	$44.47 \pm 0.17$	0.153	1.91	fsrq
J0045.1−3706	1.015	$8.61 \pm 0.41$	$45.86 \pm 0.07$	0.137	2.95	fsrq
J0049.6−4500	0.121	$8.09 \pm 0.44$	$43.51 \pm 0.15$	0.002	0.47	bll
J0133.1−5201	0.925	$8.5 \pm 0.4$	$46.32 \pm 0.05$	0.508	11.22	fsrq
J0143.5−3156	0.374	$7.45 \pm 0.05$	$44.79 \pm 0.02$	0.168	0.85	bll
J0200.6−6637	1.285	$8.25 \pm 0.2$	$45.42 \pm 0.04$	0.114	2.45	fsrq
J0204.8+1513	0.407	$7.75 \pm 0.36$	$43.83 \pm 0.16$	0.010	2.24	fsrq
J0223.5−0928	1.005	$8.37 \pm 0.24$	$45.14 \pm 0.09$	0.045	4.57	fsrq
J0226.3−1845	1.67	$7.94 \pm 0.27$	$45.78 \pm 0.07$	0.532	7.59	fsrq
J0327.5−1805	0.73	$8.04 \pm 0.22$	$44.96 \pm 0.06$	0.064	12.3	fsrq
J0340.4−2422	0.683	$9.0 \pm 0.19$	$46.25 \pm 0.03$	0.137	11.22	fsrq
J0430.2−0356	0.628	$7.82 \pm 0.06$	$45.2 \pm 0.01$	0.185	89.12	fsrq
J0516.8−0509	1.417	$8.98 \pm 0.14$	$45.85 \pm 0.05$	0.057	6.46	fsrq
J0522.9−3628	0.056	$7.79 \pm 0.28$	$43.53 \pm 0.29$	0.004	0.63	bll
J0621.2−4648	1.212	$7.72 \pm 0.33$	$45.55 \pm 0.1$	0.520	8.91	fsrq
J0622.9+3326	1.062	$8.03 \pm 0.29$	$45.5 \pm 0.08$	0.227	5.75	fsrq
J0644.4−6712	1.94	$9.26 \pm 0.38$	$45.63 \pm 0.17$	0.018	1.2	fsrq
J0658.1−5840	0.421	$7.73 \pm 0.19$	$43.71 \pm 0.06$	0.007	2.29	bll
J0725.8−0054	0.128	$8.0 \pm 0.47$	$43.58 \pm 0.29$	0.003	0.46	bll
J0728.0+6735	0.844	$8.63 \pm 0.15$	$46.13 \pm 0.03$	0.243	39.81	fsrq
J0749.3+4453	0.559	$7.43 \pm 0.26$	$44.48 \pm 0.12$	0.086	2.0	fsrq
J0821.1+1007	0.954	$7.95 \pm 0.18$	$45.35 \pm 0.07$	0.193	4.07	fsrq
J0904.0+2724	1.721	$9.01 \pm 0.16$	$46.41 \pm 0.03$	0.193	11.75	fsrq
J0904.9−5734	0.697	$8.43 \pm 0.25$	$44.7 \pm 0.06$	0.014	2.88	fsrq
J0922.7−3959	0.595	$8.51 \pm 0.24$	$45.59 \pm 0.04$	0.092	4.07	fsrq
J0941.7+4125	0.816	$8.41 \pm 0.13$	$44.86 \pm 0.04$	0.022	5.5	fsrq
J0943.7+6137	0.791	$8.42 \pm 0.06$	$45.76 \pm 0.03$	0.168	6.76	fsrq
J0949.7+5819	1.424	$8.3 \pm 0.19$	$45.31 \pm 0.08$	0.079	2.45	fsrq
J1017.8+0715	1.54	$8.86 \pm 0.05$	$45.74 \pm 0.02$	0.058	2.88	fsrq
J1018.9+1043	0.66	$7.78 \pm 0.57$	$44.05 \pm 0.38$	0.014	4.37	fsrq
J1047.9+0055	0.252	$6.59 \pm 0.02$	$43.85 \pm 0.02$	0.140	2.14	fsrq
J1054.2+3926	2.635	$8.59 \pm 0.2$	$45.78 \pm 0.06$	0.119	3.98	fsrq
J1124.4+2308	0.795	$7.86 \pm 0.2$	$44.87 \pm 0.12$	0.079	2.14	fsrq
J1129.2−0529	0.922	$7.58 \pm 0.22$	$44.91 \pm 0.06$	0.164	7.59	fsrq
J1131.4−0504	0.263	$6.77 \pm 0.47$	$43.15 \pm 0.28$	0.018	0.41	bll
J1139.0+4033	2.361	$8.99 \pm 0.09$	$46.33 \pm 0.01$	0.168	4.17	fsrq
J1159.2−2227	0.565	$8.34 \pm 0.13$	$45.02 \pm 0.13$	0.037	7.76	fsrq
J1205.8+3321	1.007	$8.37 \pm 0.06$	$45.3 \pm 0.05$	0.065	7.41	fsrq
J1214.6−1926	0.148	$7.37 \pm 0.68$	$44.62 \pm 0.03$	0.137	0.59	bll
J1243.0+3950	1.22	$8.77 \pm 0.36$	$45.65 \pm 0.04$	0.058	5.01	fsrq
J1248.9+4840	1.856	$8.11 \pm 0.25$	$45.53 \pm 0.07$	0.202	4.79	fsrq
J1319.5−0045	0.891	$8.55 \pm 0.02$	$46.08 \pm 0.01$	0.261	1.62	fsrq
J1323.0+2941	1.142	$8.82 \pm 0.27$	$44.62 \pm 0.07$	0.005	9.33	bll
J1329.4−0530	0.576	$9.22 \pm 0.19$	$46.31 \pm 0.07$	0.095	2.29	fsrq
J1412.9+5018	1.53	$8.37 \pm 0.07$	$45.55 \pm 0.05$	0.116	4.68	fsrq
J1418.4+3543	0.825	$7.83 \pm 0.38$	$44.84 \pm 0.06$	0.079	16.59	fsrq
J1454.0+4927	2.106	$8.4 \pm 0.1$	$46.17 \pm 0.04$	0.453	5.62	fsrq

**Table 2.** Continued.

4FGL name	$z$	$M_{\text{BH}}$	$L_{\text{disk}}$	$L_{\text{disk}}/L_{\text{Edd}}$	CD	Classification
J1615.6+2130	1.627	$8.04 \pm 0.16$	$45.7 \pm 0.03$	0.352	14.45	fsrq
J1627.3+4758	2.32	$8.67 \pm 0.14$	$45.65 \pm 0.06$	0.073	3.55	fsrq
J1720.2+3824	0.454	$7.93 \pm 0.7$	$44.36 \pm 0.1$	0.021	7.94	fsrq
J1816.9–4942	1.7	$8.76 \pm 0.52$	$45.75 \pm 0.12$	0.075	4.57	fsrq
J1821.6+6819	1.69	$8.9 \pm 0.12$	$46.1 \pm 0.07$	0.122	14.79	fsrq
J2136.2–0642	0.941	$8.35 \pm 0.03$	$45.84 \pm 0.01$	0.238	1.29	fsrq
J2140.5–6731	2.009	$8.36 \pm 0.79$	$45.75 \pm 0.11$	0.189	13.49	fsrq
J2211.2–1325	0.392	$8.47 \pm 0.16$	$45.56 \pm 0.05$	0.095	2.24	fsrq
J2253.3+3233	0.257	$7.73 \pm 0.13$	$44.59 \pm 0.05$	0.056	0.54	bll
J2259.7–3549	0.754	$8.02 \pm 0.19$	$45.14 \pm 0.05$	0.101	3.72	fsrq
J2311.7+2604	1.748	$8.12 \pm 0.11$	$45.61 \pm 0.05$	0.238	3.39	fsrq
J2313.9–4501	2.877	$8.76 \pm 0.2$	$46.25 \pm 0.05$	0.238	4.79	fsrq
J2318.2+1915	2.163	$7.76 \pm 0.07$	$45.85 \pm 0.03$	0.946	39.81	fsrq
J2326.2+0113	1.6	$9.29 \pm 0.28$	$45.18 \pm 0.1$	0.006	1.32	bll
J2334.9–2346	0.048	$8.32 \pm 0.28$	$43.47 \pm 0.08$	0.001	0.59	bll
J2338.1+0325	0.269	$7.87 \pm 0.15$	$43.82 \pm 0.17$	0.007	1.1	bll
J2339.6+0242	2.661	$9.05 \pm 0.05$	$46.19 \pm 0.06$	0.106	25.7	fsrq
J2352.9+3031	0.876	$8.05 \pm 0.13$	$45.01 \pm 0.08$	0.070	3.63	fsrq

Other information are same as Table 1.

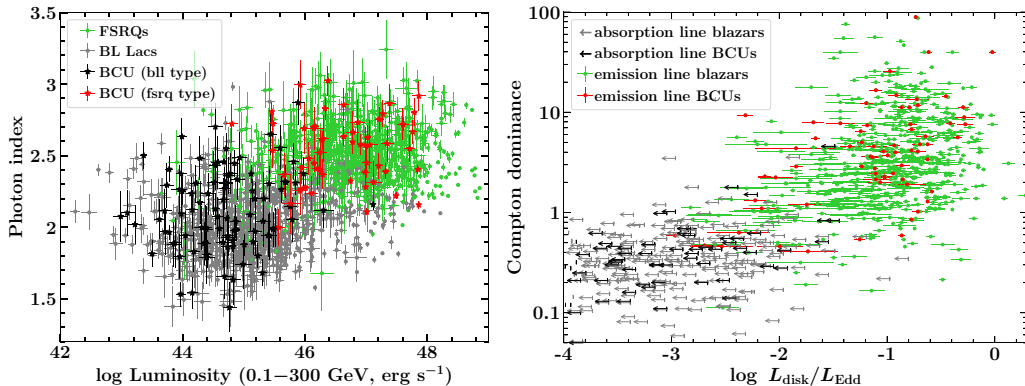


**Figure 2.** Left: The  $\gamma$ -ray luminosity versus  $\gamma$ -ray photon index plane for *Fermi*-LAT detected blazars. The BCUs classified as FSRQs/BL Lacs tend to occupy the region populated mainly by known FSRQs/BL Lacs, supporting the classification scheme. Right: The Compton dominance versus accretion disk luminosity in Eddington units.

identified as BL Lac type sources. This result further supports the blazar classification scheme proposed by Paliya *et al.* (2021).

The right panel of Figure 2 shows the variation of the Compton dominance as a function of the accretion luminosity in Eddington units. A majority of emission line BCUs have radiatively efficient accretion, i.e., their accretion luminosity is  $\geq 1\%$  of the Eddington luminosity. Furthermore, a few of them do exhibit low-level accretion activity and probably belong to the BL Lac class (see Table 2). It is possible that optical spectra of such blazars were taken during the low jet activity state,

revealing the faint emission lines similar to the prototype of this class BL Lac itself (Vermeulen *et al.* 1995). Finally, BCUs identified in this work appear to follow the positive correlation between the plotted quantities as found by Paliya *et al.* (2021) for other blazars.

#### 4. Summary

Taking the advantage of the recently published optical spectral parameters and Compton dominance computed from the multi-wavelength SEDs (Paliya *et al.*

2021), this work classifies 153 *Fermi* BCUs. Among the whole sample, 57 are found to exhibit FSRQs type behavior and the remaining 96 may belong to the BL Lac population. The results obtained also support the hypothesis that the Compton dominance can be used as a proxy for the accretion rate in Eddington units. Since current and next-generation all-sky surveys, e.g., e-ROSITA, and Square Kilometer Array, are going to provide flux measurements across the electromagnetic spectrum, a precise measurement of the Compton dominance would be possible for a large sample of blazars. In this regard, a Compton dominance-based blazar classification scheme can be very useful in identifying the FSRQ/BL Lac nature of BCUs, enabling a better understanding of the physics of relativistic jets.

## References

- Ackermann M., Ajello M., Allafort A., *et al.* 2011, ApJ, 743, 171, <https://doi.org/10.1088/0004-637X/743/2/171>
- Ahumada R., Allende Prieto C., Almeida A., *et al.* 2020, ApJS, 249, 3, <https://doi.org/10.3847/1538-4365/ab929e>
- Ajello M., Angioni R., Axelsson M., *et al.* 2020, ApJ, 892, 105, <https://doi.org/10.3847/1538-4357/ab791e>
- Cappellari M., Emsellem E. 2004, PASP, 116, 138, <https://doi.org/10.1086/381875>
- Ghisellini G., Tavecchio F., Foschini L., Ghirlanda G. 2011, MNRAS, 414, 2674, <https://doi.org/10.1111/j.1365-2966.2011.18578.x>
- Giommi P., Padovani P., Polenta G. 2013, MNRAS, 431, 1914, <https://doi.org/10.1093/mnras/stt305>
- Gültekin K., Richstone D. O., Gebhardt K., *et al.* 2009, ApJ, 698, 198, <https://doi.org/10.1088/0004-637X/698/1/198>
- Paliya V. S., Domínguez A., Ajello M., Olmo-García A., Hartmann D. 2021, ApJS, 253, 46, <https://doi.org/10.3847/1538-4365/abe135>
- Paliya V. S., Domínguez A., Cabello C., *et al.* 2020, ApJL, 903, L8, <https://doi.org/10.3847/2041-8213/abbc06>
- Peña-Herazo H. A., Amaya-Almazán R. A., Massaro F., *et al.* 2020, A&A, 643, A103, <https://doi.org/10.1051/0004-6361/202037978>
- Shen Y., Richards G. T., Strauss M. A., *et al.* 2011, ApJS, 194, 45, <https://doi.org/10.1088/0067-0049/194/2/45>
- Stickel M., Padovani P., Urry C. M., Fried J. W., Kuehr H. 1991, ApJ, 374, 431, <https://doi.org/10.1086/170133>
- Vermeulen R. C., Ogle P. M., Tran H. D., *et al.* 1995, ApJL, 452, L5, <https://doi.org/10.1086/309716>